Study of fast electron generation using multi beam of LFEX-class laser

Journal of Physics: Conference Series **717** (2016) 012037 doi:10.1088/1742-6596/717/1/012037

Study of fast electron generation using multi beam of LFEX-class laser

M Hata[1], H Sakagami[2], T Johzaki[3], Y Sentoku[4] and H Nagatomo[1]

[1]Institute of Laser Engineering, Osaka University, Suita, Osaka 565-0871, Japan
[2]Fundamental Physics Simulation Research Division, National Institute for Fusion Science, Toki, Gifu 509-5292, Japan
[3]Graduate School of Engineering, Hiroshima University, Higashihiroshima, Hiroshima 739-8527, Japan
[4]Department of Physics, University of Nevada, Reno, Nevada 89557, USA

E-mail: masayasuhata@gmail.com

Abstract. Fast Ignition Realization Experiment project phase-I (FIREX-I) is being performed at Institute of Laser Engineering, Osaka University. In this project, the four-beam bundled high-energy Petawatt laser (LFEX) is being operated. LFEX laser provides great multi-beam irradiation flexibility, with the possibility of arrange the pulses in temporal sequence, spatially separate them in distinct spots of focus them in a single spot. In this paper, we study the two-beam interference effects on high-intensity picosecond laser-plasma interaction (LPI) by two-dimensional relativistic Particle-In-Cell simulations. The interference causes surface perturbation, which enhances laser absorption and underdense plasma generation, increasing the accelerated electron number and their slope temperature. The laser-to-electron energy conversion efficiency for two-beam interference case is suitable for Fast Ignition (FI) compared to the single beam case, but the increment of fast electron divergence leads to lower energy coupling. To optimize the target design for FI, these interference effects should be taken into consideration.

1. Introduction

Fast Ignition Realization Experiment project phase-I (FIREX-I) is being performed at Institute of Laser Engineering [1,2], Osaka University. In this project, the four-beam bundled high-energy petawatt laser (LFEX) is being operated [3]. LFEX laser provides great multi-beam irradiation flexibility, with the possibility of arrange the pulses in temporal sequence, spatially separate them in distinct spots of focus them in a single spot. In case of no beam overlapping, the maximum beam energy, and consequently intensity, is limited by the maximum allowed energy for a single beam. In contrast, in case of beam overlapping the laser intensity on target is increased, but the beams undergo interference. According to previous computational research [4], the spatially overlapped irradiation causes the generation of structures on the target plasma surface according to the interference pattern and therefore affecting the laser-plasma interaction. However, scale-down parameters are used in this study, e.g. the pulse duration is less than 700 femtoseconds and the spot diameter (FWHM) is set to 10 μm. Features of the LFEX, which are high power, long pulse, and spot diameter much larger than the diffraction limit, are considered to provide interesting results that differ from many usual research

works, where the laser is ultrahigh intensity, but much shorter pulses and close to diffraction limit spot sizes. Kemp et al. [5] reported that a high-power long-pulse laser such as LFEX creates a large underdense plasma during irradiation which in turn affects the LPI resulting in a increment of the hot electron temperature even with no initial pre-plasma. Therefore, large-scale simulations using realistic laser and target parameters are strongly desired. In this paper, we study the two-beam interference effect on high-intensity LPI by two-dimensional relativistic Particle-In-Cell simulations using PICLS2D code [6].

2. Simulation of multi beam irradiation to planar target

Two-dimensional Particle-In-Cell simulations of Petawatt-class laser irradiation of a planar target have been carried out. The target is simulated as a simple 20 μm Au plasma with uniform electron density of $40n_{cr}$ and an exponentially decreasing, 1μm scale-length pre-plasma extending from 0.1 to $40n_{cr}$, where n_{cr} is the critical electron density.

The choice of such short pre-plasma scale-length is justified because we are assuming a high contrast laser pulse, following the recent upgrades of LFEX laser. Fixing the total laser energy, two laser profile conditions are chosen: one-beam irradiation and two-beam irradiation which intensity per beam is half the intensity of the single beam case. The temporal profile of each beam at the focus is expressed by $I(r,t) = I_0 \exp\left(-\frac{r^2}{r_0^2}\right) \exp\left[-\frac{(t-3t_0)^2}{2t_0^2}\right]$, where r_0 = 25λ_L and t_0 = 191($2\pi/\omega_L$), corresponding to 41.6 μm FWHM spot size and 1500 fs FWHM pulse duration for 1 μm wavelength. The peak intensities of the laser beam are set to be 1.36×10^{19} Wcm^{-2} for one-beam irradiation and 6.8×10^{18} Wcm^{-2} for two-beam irradiation, keeping the same total laser energy. The laser is focused at the center of the target surface, namely (x,y) = (105 μm,72 μm) in fig 1(b). Laser incidence angle is normal for one-beam irradiation and tilted by ± 2.86 degrees for two-beam irradiation.

2.1. Effects of interference

Figure 1 shows two-dimensional spatial profile of (a) square of the electric field and (b) electron density for (1) one- and (2) two-beam irradiation at 2228 fs , close to the time of peak laser irradiation on the plasma surface. In fig. 1(a-2), apparent interference pattern can be observed with interval of about 10 μm. Considering interference of two plane waves, the interference pattern interval is expressed by $l_{\text{interference}} = \frac{1}{2}\frac{\lambda_L}{\sin\theta}$, where λ_L is the wavelength and θ is the half of angle between two waves, and it is calculated to be 10.0 μm using simulated parameters of λ_L = 1 μm and θ = 2.86 degrees, in agreement with the observed interval. Laser interference generates a periodic intensity pattern at specific points with hole boring occurring at high-intensity irradiation areas, correspondingly generating a periodic surface structure as shown in fig. 1(b-2).

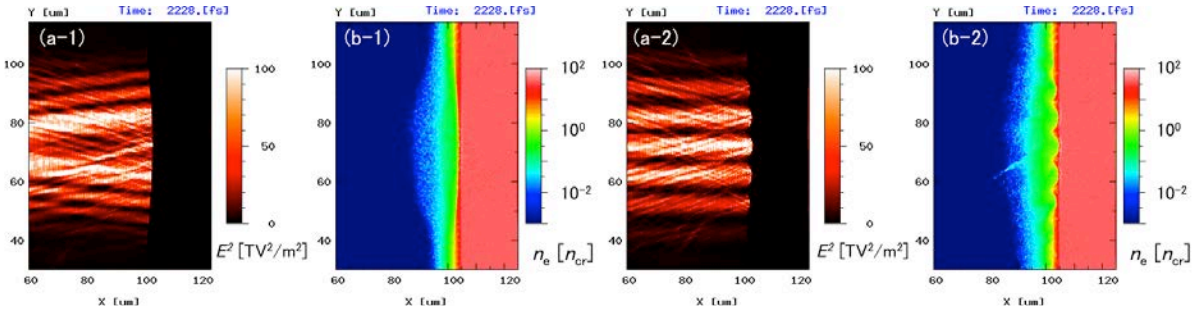

Figure 1. 2-D spatial profile of (a) square of electric field and (b) electron density in the cases of (1) one-beam and (2) two-beam irradiation at 2228 fs, namely around the time of laser peak intensity.

Figure 2 shows cross sections of the electric field (E_y) profile along x-axis at 2228 fs, where red and green lines represent the cross sections in case of one and two-beam irradiation and solid and dashed lines indicate those of Y = 72 and 67 μm, respectively. For two-beam irradiation, maximum electric field is around 20 TV/m, twice the maximum electric field for one-beam irradiation. Figure 3 shows cross sections of the electron density profile along the x-axis, where black solid line indicates initial density, red and green solid lines represent the profiles at 2228 fs respectively in case of one- and two-beam irradiation along the focal spot centerline (Y = 72μm), while dashed red and green lines indicate the profiles 5 μm below centerline (Y = 67 μm) respectively. For one-beam irradiation, electron density profiles are similar both at Y = 72 and 67 μm. On the other hand, a large difference is observed for electron density profiles at Y = 72 and 67 μm in two-beam irradiation. For the latter case in fact the laser irradiated surface is prominently compressed inwards at Y = 72 μm compared to the one-beam case. In contrast, at Y = 67 μm a larger underdense plasma blown-off is observed for the two beam case compared to the one beam case, although the electron profile above critical density does not significantly differ from initial density profile. These features may affect the parameters of the generated fast electron distribution.

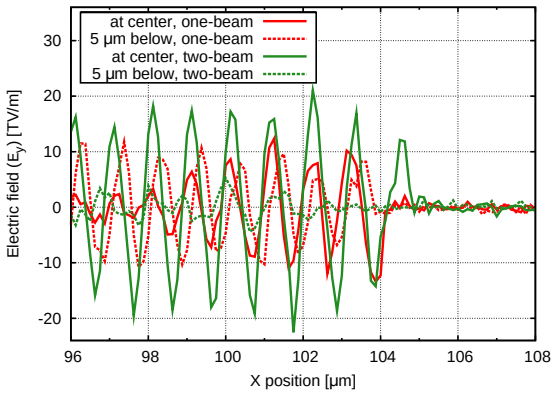

Figure 2. Cross sections of electric field (E_y) profile along x axis at 2228 fs, where red and green lines represent respectively the cross sections for one- and two-beam irradiation case, solid and dashed lines indicate respectively profiles taken at Y = 72 and 67 μm.

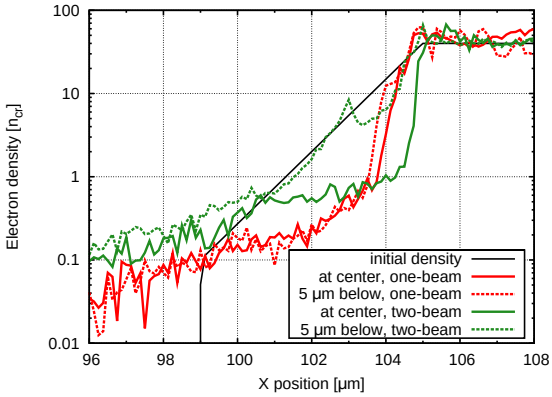

Figure 3. Cross sections of electron density profile along x axis, where black solid line indicates initial density, red and green lines represent profiles at 2228 fs in case of one- and two-beam irradiation, solid and dashed lines indicate profiles taken at Y = 72 and 67 μm, respectively.

2.2. Fast electron characteristics

Fast electron parameters are measured at the X=115 μm plane. Figure 4 shows the time-integrated fast electron energy spectrum. A larger number of fast electrons is generated in the two-beam irradiation compared to the one-beam irradiation case, with slope temperature estimated to be 2.4 and 2.8 MeV for one- and two-beam irradiation respectively. This result can be explained by the generation of large pre-plasma and surface structure in the two-beam irradiation case. The surface modulation at relativistic critical density increases the area where the laser incidence is oblique. Reflected laser light is measured on the plane at X = 0 μm and the calculated absorption rates are about 47% and 80 % respectively for the one and two beam irradiation case at the end of simulation. Consequently enhanced fast electron generation for two beam interference case is observed, as shown in Figure 4.

The half-angle fast electron angular divergence, (HWHM of the fast electron angular distribution) as function of the electron energy is shown in figure 5. The fast electron divergence for two-beam irradiation is larger than for one-beam case over whole energy range. Because of surface modulation at relativistic critical density, the number of obliquely propagating fast electrons increase. In addition, the

hgh intensity fields modulated over the interference pattern locally generate high currents and large magnetic fields. These magnetic fields enhance the divergence of relatively low-energy electrons.

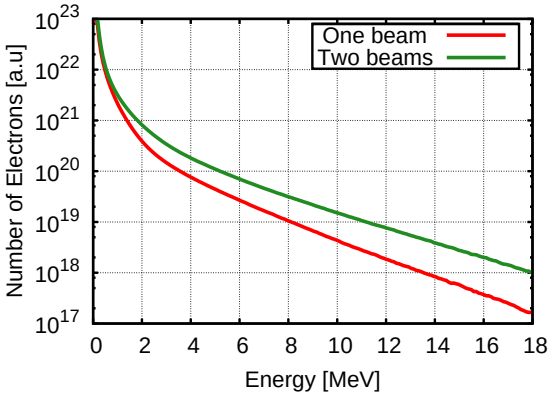

Figure 4. Time-integrated energy spectrum of fast electrons passing through X = 115 μm.

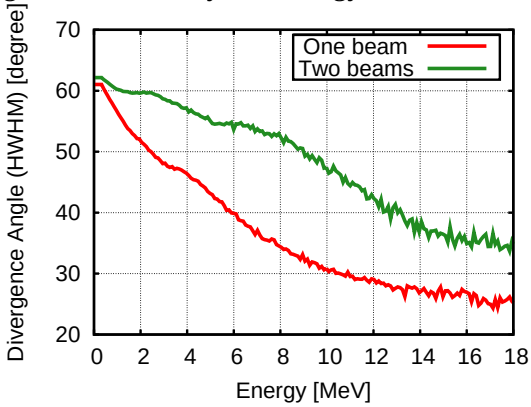

Figure 5. Divergence angle (HWHM) of observed fast electrons in momentum space.

3. Summary

Two-dimensional PIC simulation using realistic parameters of LFEX laser were performed and effects of beam interference were investigated. The interference induces surface perturbations, which enhance the laser absorption and the creation of underdense plasma, increasing the generated fast electron number and the relative slope temperature. On the other hand, the surface perturbation also cause wider fast electrons divergence. From a fast ignition point of view, large fast electron divergence leads to lower coupling efficiency to the fuel core, but at the same time high absorption leads to higher coupling efficiency. Simply, a large divergence angle does not significantly affect the coupling efficiency if the core is located near the fast electrons generation point, but it strongly affects it if the core is far from the fast electron generation point. Fast electron guiding via external, laser-generated magnetic fields may solve the disadvantage of interference effects [7]. To optimize the target design for fast ignition, these conflicting effects, namely effects of higher absorption and wider fast electron divergence due to interference, should be clarified via full-scale PIC-Hybrid-Hydro simulation under the realistic conditions, including implosion, fast electron generation, and core heating processes.

Acknowledgments

This work was supported by JSPS Grant-in-Aid (No. 15K17798) and NIFS Collaboration Research program (NIFS12KUGK057 and NIFS14KNSS054).

References

[1] H. Azechi and the FIREX Project, Plasma Phys. Controlled Fusion **48**, B267 (2006).
[2] H. Azechi, et al., Nucl. Fusion **53**, 104021 (2013).
[3] N. Miyanaga *et al., J. Physique IV France* **133**, 81 (2006)
[4] H. Sakagami, et al., Proc. 39th EPS Conf. on Plasma Physics P2.122 (2012)
[5] A. J. Kemp and L. Divol, Phys. Rev. Lett. **109**, 195005 (2012).
[6] Y. Sentoku and A. J. Kemp, J. Comput. Phys. **227**, 6846 (2008).
[7] T. Johzaki, et al., Nucl. Fusion **55**, 053022 (2015).